Targeting and Suppression of Survivin in Cancer Cells Based on the Interaction of Cell Surface Vimentin with N-Acetylglucosamine-Bearing Polymers

Kitagawa, Karera
Applied Chemistry, Graduate School of Engineering, Kyushu University

Kobayashi, Shingo
Institute for Materials Chemistry and Engineering, Kyushu University

Miura, Yoshiko
Chemical Engineering, Graduate School of Engineering, Kyushu University

Tanaka, Masaru
Institute for Materials Chemistry and Engineering, Kyushu University

他

ACS OMEGA

Open Access

http://pubs.acs.org/journal/acsodf

Article

Targeting and Suppression of Survivin in Cancer Cells Based on the Interaction of Cell Surface Vimentin with *N*-Acetylglucosamine-Bearing Polymers

Karera Kitagawa, Shingo Kobayashi,* Yoshiko Miura, Masaru Tanaka, and Hirohiko Ise*

Cite This: https://doi.org/10.1021/acsomega.5c02098

Read Online

ACCESS | Metrics & More | Article Recommendations | Supporting Information

ABSTRACT: Survivin, a protein overexpressed in various fetal and malignant tumor tissues, induces tumor progression and resistance to cancer therapy. Cell surface vimentin has *N*-acetylglucosamine (GlcNAc)-binding activities in several cell types including tumor cells. Furthermore, GlcNAc-bearing polymers downregulate the expression of the survivin-encoding baculoviral inhibitor of apoptosis protein repeat-containing protein 5 (*BIRC5*). Thus, cell surface vimentin is a target for cancer therapy. The downregulation of survivin expression in cancer cells by selectively targeting cell surface vimentin with GlcNAc-bearing polymers may mitigate drug resistance. However, the ability of GlcNAc to bind to cell surface vimentin depends on its valency in GlcNAc-bearing polymers. The optimal GlcNAc valency for the interaction remains unknown. Therefore, we aimed to develop optimal GlcNAc-bearing polymers for effective cancer therapy. In this study, GlcNAc polymers of various lengths were synthesized through reversible addition/fragmentation chain-transfer polymerization. We found that a low-molecular-weight GlcNAc polymer (5 GlcNAc-mer) interacted with cell surface vimentin-expressing cells to a greater extent than high-molecular-weight GlcNAc polymers (10 and 20 GlcNAc-mer). These interactions upregulated the expression of p53, an upstream signal transducer. Moreover, they inhibited the phosphorylation of signal transducers and activators of transcription 3 and downregulated survivin expression. In addition, low-molecular-weight GlcNAc polymers decreased the viability of 3LL cells, mouse lung carcinoma cell lines, and MCF-7 cells, human breast cancer lines, but not that of MCF10A, nontumorigenic breast cells. These findings suggest that low-molecular-weight GlcNAc polymers, which selectively target cancer cells and downregulate survivin expression, are promising tools for cancer therapy.

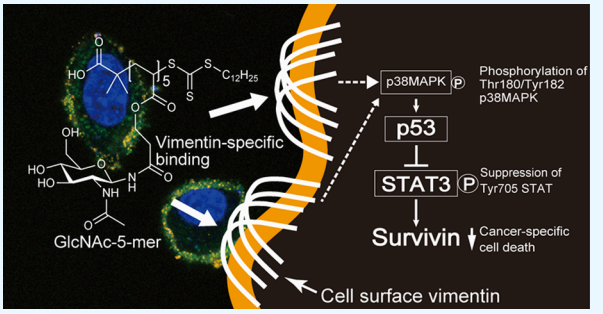

INTRODUCTION

Survivin, also known as baculoviral inhibitor of apoptosis protein (IAP) repeat-containing protein 5, is a 16 kDa protein that belongs to the IAP family.[1−6] This molecule is highly expressed in fetal and malignant tumor tissues.[2,4−9] In addition, it regulates cell-cycle progression and prevents apoptosis. This protein is not expressed in adult differentiated tissues other than adult stem cells, where it maintains stemness.[2,4−6,9] Moreover, survivin is specifically overexpressed in tumor tissues; it induces tumor progression and resistance to various antitumor therapies, such as chemotherapy and radiotherapy.[1−3,6−9] Therefore, survivin is an attractive target for antitumor therapies. The inhibition of this protein along with the downregulation of its expression in tumor tissues may be a promising treatment approach. Many survivin-inhibiting approaches in tumor tissues, such as the delivery of survivin-siRNA and low-molecular-weight compounds such as YM155, have been developed.[3,6,9,10] However, survivin-siRNA is of high molecular weight, and survivin-inhibiting low-molecular-weight compounds do not have selectivity for cancer tissues. Thus, difficulties in the delivery of survivin-siRNA and the side effects of the compounds remain major concerns.

Our previous study revealed the *N*-acetylglucosamine (GlcNAc)-binding properties of cell surface vimentin. Various cells that express vimentin on the surface, such as tumor cells, fibroblasts, and mesenchymal stem cells, can interact with GlcNAc-bearing polymers.[11−16] Moreover, the interaction of GlcNAc-bearing polymers with cell surface vimentin regulates the expression of various genes in fibroblasts.[13] This interaction suppresses proliferation- and cell-cycle progression-related genes. In particular, the addition of GlcNAc-bearing polymers to fibroblasts induces the expression of p53, a tumor suppressor gene. In addition, it substantially reduces survivin levels.[13] These alterations in gene expression are

Received: March 6, 2025
Revised: July 30, 2025
Accepted: August 8, 2025

Table 1. Polymerization of CEA-GlcNAc and AES-GlcNAc Monomers Using RAFT Agents[a]

entry	polymers	RAFT agents	RT (h)	ratio (mol %) [monomer]:[RAFT agent]:[initiator]	conv.[b] (%)	yield (%)	M_n[c] (g/mol)	M_w[c] (g/mol)	M_w/M_n[c]	DP[b]
1	pCEA-GlcNAc5	DDMAT	1.5	6.25:1:0.2	80	49	1900	2200	1.2	5
2	pCEA-GlcNAc10	DDMAT	1.5	12.5:1:0.2	66	27	3100	4100	1.4	10
3	pCEA-GlcNAc20	DDMAT	4	25:1:0.2	96	87	5400	7300	1.4	22
4	pAES-GlcNAc5	DDMAT	24	6.25:1:0.2	>99	59	1900	2600	1.4	5
5	pAES-GlcNAc10	DDMAT	24	12.5:1:0.2	>99	32	4600	6200	1.4	9
6	pAES-GlcNAc20	DDMAT	24	25:1:0.2	>99	70	9100	12,700	1.4	19
7	DBD-ED-pCEA-GlcNAc5	DBD-ED-CDTPA	24	6.25:1:0.2	94	63	2000	2400	1.2	4
8	DBD-ED-pCEA-GlcNAc10	DBD-ED-CDTPA	24	12.5:1:0.2	93	78	3100	3900	1.3	10

[a]The monomer concentration for each polymerization was set to 0.5 mol/L, and the reaction time (RT) was set to 1.5−24 h. The ratio was [Monomer]:[RAFT agent]:[Initiator] = 1.25 × n:1:0.2; n indicates the target degree of polymerization. [b]Conversion (Conv.) and degree of polymerization (DP) were determined using ^{1}H NMR. [c]The relative weight-average molecular weight (M_w), number-average molecular weight (M_n), and polydispersity index (M_w/M_n) were determined through GPC analysis calibrated with a pullulan standard. The eluent was 20% acetonitrile/200 mmol/L $NaNO_3$ solution.

caused by the activation of p38 mitogen-activated protein kinase (MAPK) and suppression of the phospho-signal transducer and activator of transcription 3 when cell surface vimentin interacts with GlcNAc-bearing polymers.[13] Vimentin belongs to the type III intermediate filament family and maintains cellular architecture and shape in intracellular areas.[17] However, it is expressed on the surface of highly malignant tumor cells such as circulating tumor cells. Thus, it has been identified as a marker of these cells.[18−21] Therefore, GlcNAc-bearing polymers may be used to target cancer cells. Moreover, the interaction of various cancer cells with GlcNAc-bearing polymers via cell surface vimentin could downregulate survivin overexpression. The downregulation of survivin expression in cancer cells is highly advantageous for chemotherapy because it can mitigate the drug resistance associated with this protein.[22]

The structural requirements for the interaction of GlcNAc-bearing polymers with cancer cells through cell surface vimentin must be determined to achieve a high therapeutic efficacy against cancer. The carbohydrate structure must be adjusted to facilitate strong interactions between glycopolymers and carbohydrate-binding proteins such as lectins.[23] In this study, GlcNAc monomers of different sizes and GlcNAc-bearing polymers of different lengths were designed to construct GlcNAc-bearing polymers that can strongly interact with vimentin-expressing cancer cells. We specifically targeted cancer cells and reduced survivin expression using the strong interaction of these GlcNAc-bearing polymers with cell surface vimentin. Based on our findings, we propose a novel cancer therapy that inhibits survivin expression to mitigate drug resistance.

EXPERIMENTAL SECTION

Materials. GlcNAc, activated charcoal, methanol with ammonia, mono(2-acryloyloxyethyl) succinate, 4-methoxyphenol (MEHQ), 2-(dodecylthiocarbonothioylthio)-2-methylpropionic acid (DDMAT), 2,2′-azobis(isobutyronitrile) (AIBN), 4-cyano-4-[[(dodecylthio) carbonothioyl]thio] pentanoic acid (CDTPA), and 4-(*N*,*N*-dimethylaminosulfonyl)-7-(2-aminoethylamino)-2,1,3-benzoxadiazole (DBD-ED) were purchased from Tokyo Chemical Industry Co., Ltd. (Tokyo, Japan). Methanol, chloroform, dimethyl sulfoxide (DMSO), sodium nitrate, accutase, penicillin/streptomycin, Dulbecco's modified Eagle's medium (DMEM) (high glucose), minimum essential medium (MEM) (high glucose), 100 mmol/L-sodium pyruvate solution (100×), antibiotics/antimycotics, paraformaldehyde, Fluoro-KEEPER Antifade Reagent Non-Hardening Type with DAPI, protease inhibitor cocktail, phosphatase inhibitor cocktail, Blocking One, Signal Enhancer HIKARI, insulin (human, recombinant, expressed in yeast, animal-free), and cell counting reagent SF were purchased from NACALAI TESQUE Inc. (Kyoto, Japan). Mammary epithelial cell growth medium (MEGM) BulletKit was purchased from the Lonza Group AG. (Basel, Switzerland). Acetonitrile, Leibovitz's L15 medium, and Hank's balanced salt solution (HBSS) were obtained from Thermo Fisher Scientific Inc. (Waltham, MA, USA). Amberlyst 15, 2-carboxyethyl acrylate, Super-DHB, and cholera toxin were purchased from Sigma-Aldrich (St. Louis, MO, USA). 4-(4,6-Dimethoxy-1,3,5-triazin-2-yl)-4-methylmorpholinium chloride (DMT-MM) was obtained from KOKUSAN CHEMICAL Co., Ltd. (Tokyo, Japan). Hexane, deuterium oxide (D_2O), sodium 3-(trimethylsilyl) propionate-2,2,3,3-d_4 (TMS), and polyoxyethylene sorbitan monolaurate (Tween-20) were obtained from FUJIFILM Wako Pure Chemical Corporation (Osaka, Japan). DMSO-d_6 was obtained from EurIsotop. Puromycin was purchased from InvivoGen (San Diego, CA, USA). Spectra/Por 6 Dialysis Membrane Prewetting RC Tubing was obtained from Repligen Corporation (Waltham, MA, USA). CF555 donkey antirabbit IgG (H + L) was obtained from Biotium Inc. (San Francisco, CA, USA). Immobilon-P PVDF membranes and Immobilon Forte Western HRP substrates were obtained from Merck Millipore (Darmstadt, Germany). The 48- and 96-well plates were obtained from IWAKI AGC TECHNO GLASS Co., Ltd. (Shizuoka, Japan). 3LL cells were purchased from the National Institute of Biomedical Innovation, Health, and Nutrition (Osaka, Japan). HeLa cells were obtained from a RIKEN BRC (Tsukuba, Japan). Survivin (71G4B7) rabbit monoclonal antibody was purchased from Cell Signaling Technology (Danvers, MA, USA). P53 rabbit polyclonal antibody (21891-1-AP), STAT3 rabbit polyclonal antibody (10253-2-AP), and β-actin monoclonal antibody (66009-1-Ig) were purchased from Proteintech (Rosemont, IL, USA). Anti-STAT3 (phospho Y705) antibody (EP2147Y) (ab76315) was purchased from Abcam (Cambridge, UK). Horseradish peroxidase (HRP)-conjugated donkey polyclonal antirabbit IgG (715-035-152) and HRP-conjugated donkey polyclonal antimouse IgG (715-035-153) were obtained from Jackson

https://doi.org/10.1021/acsomega.5c02098
ACS Omega XXXX, XXX, XXX−XXX

ImmunoResearch Inc. (West Grove, PA, USA). Shodex STANDARD P-82 was obtained from Showa Denko K.K. (Tokyo, Japan).

Nuclear Magnetic Resonance Measurement. NMR (^{1}H NMR, ^{13}C NMR, DEPT135, ^{1}H−^{1}H COSY, and ^{1}H−^{13}C HMQC) spectra were recorded using a Bruker AVANCE III 400 or 600 MHz CryoProbe. The NMR spectra were recorded at 298 K in D_2O or DMSO-d_6. Chemical shifts (δ) and coupling constants (J) are reported in parts per million and Hertz (Hz), respectively. The proton chemical shifts were referenced to D_2O (4.79 ppm) and DMSO-d_6 (2.50 ppm). Multiplicity in the ^{1}H NMR spectra is described as singlet (s), doublet (d), doublet of doublets (dd), doublet of doublet of doublets (ddd), doublet of quartets (dq), triplet (t), multiplet (m), broad singlet (br), broad singlet (brs), and broad triplet (brt). The carbon chemical shifts were referenced to TMS (0 ppm).

Synthesis of 1-Amino GlcNAc (GlcNAc-NH$_2$). GlcNAc (40 g, ca. 180 mmol) and saturated ammonium hydrogen carbonate were added to 200 mL of water and stirred at 35 °C for 3 days.[24,25] Thin-layer chromatography was performed using a development solvent with a volume ratio of [ethyl acetate]:[acetic acid]:[methanol]:[water] of 4:3:3:1 to monitor reaction progress. After the reaction was complete, ammonium hydrogen carbonate was removed through repeated water evaporation using a rotary evaporator until no more bubbles appeared. Amberlyst 15 (40 g) was then added to the solution, and the mixture was stirred for 1 h. This was then packed into a column, and the impurities were eluted by flowing 500 mL of methanol. The target product was eluted by flowing 400 mL of methanol with ammonia (0.5 mol/L) and methanol (100 mL). Activated charcoal was added to the eluate, and the mixture was stirred at 30 °C for 1 h to further purify the product. The solution was then filtered and concentrated. GlcNAc-NH$_2$ (12.5 g, 56.8 mmol, yield = 31%) was obtained as a white solid. The product was lyophilized and stored at 4 °C.

^{1}H NMR (400 MHz, D_2O): δ = 4.15 (d, J = 9.2 Hz, 1H), 3.89 (d, J = 12.2 Hz, 1H), 3.71 (ddd, J = 12.3, 4.1, 1.8 Hz, 1H), 3.62 (dd, J = 10.1, 9.1 Hz, 1H), 3.57−3.49 (m, 1H), 3.42 (m, 2H), 2.05 (s, 3H).

^{13}C NMR (101 MHz, D_2O): δ = 177.33, 86.93, 79.54, 77.26, 72.83, 63.62, 59.12, 25.07.

FAB−MS: m/z calcd for $C_8H_{17}N_2O_5$: 221.1137; found: 221.1145.

Synthesis of GlcNAc-Linked 2-Carboxyethyl Acrylate (CEA-GlcNAc). 2-Carboxyethyl acrylate was purified through vacuum distillation (bp = 70−90 °C/0.08 Torr). A solution comprising DMT-MM (1 equiv) and 2-carboxyethyl acrylate (1 equiv) as well as small amounts (∼100 ppm) of MEHQ in methanol (10 mL) was added to GlcNAc-NH$_2$ (4.03 g, 18.3 mmol) in methanol (30 mL). The reaction mixture was then stirred at approximately 25 °C for 3 h. The solvent was removed using a rotary evaporator, and the residue was dispersed in chloroform. The precipitate was collected via suction filtration, dissolved in water, and purified using high-performance liquid chromatography (HPLC). HPLC was performed using an LC-91 × 0G NEXT column (Japan Analytical Industry) equipped with a JAIGEL-ODS-BP SP-120-15 column (Japan Analytical Industry). CEA-GlcNAc was obtained as a white solid (2.05 g, 5.94 mmol, yield = 32.4%). The product was lyophilized and stored at 4 °C.

^{1}H NMR (600 MHz, D_2O): δ = 6.45 (dd, J = 17.3, 1.1 Hz, 1H), 6.20 (dd, J = 17.3, 10.6 Hz, 1H), 6.02 (dd, J = 10.6, 1.1 Hz, 1H), 5.12 (d, J = 9.7 Hz, 1H), 4.44 (dq, J = 14.9, 5.9 Hz, 2H), 3.91 (dd, J = 12.4, 2.1 Hz, 1H), 3.85 (t, J = 10.0 Hz, 1H), 3.78 (dd, J = 12.4, 5.0 Hz, 1H), 3.64 (dd, J = 10.2, 8.6 Hz, 1H), 3.57−3.48 (m, 2H), 2.72 (t, J = 5.8 Hz, 2H), 2.02 (s, 3H).

^{13}C NMR (151 MHz, D_2O): δ = 174.66, 174.17, 168.16, 132.65, 127.32, 78.33, 77.62, 74.23, 69.48, 60.90, 60.52, 54.33, 35.01, 22.07.

FAB−MS: m/z calcd for $C_{14}H_{23}N_2O_8$: 347.1454; found: 347.1452.

Synthesis of GlcNAc-Linked Mono(2-acryloyloxyethyl) Succinate (AES-GlcNAc). AES-GlcNAc was synthesized similarly to CEA-GlcNAc. Briefly, 4.42 g (20.1 mmol) of GlcNAc-NH$_2$, DMT-MM (1.5 equiv), mono(2-acryloyloxyethyl) succinate (1.5 equiv), small amounts (∼100 ppm) of MEHQ, and 40 mL of methanol were used. After purification, AES-GlcNAc (4.15 g, 9.94 mmol, yield = 49.5%) was obtained as a white solid.

^{1}H NMR (600 MHz, D_2O): δ = 6.48 (dd, J = 17.4, 1.0 Hz, 1H), 6.25 (ddd, J = 17.4, 10.5, 0.8 Hz, 1H), 6.04 (dd, J = 10.5, 0.9 Hz, 1H), 5.08 (d, J = 8.9 Hz, 1H), 4.49−4.40 (m, 4H), 3.91 (dd, J = 12.4, 1.3 Hz, 1H), 3.85 (t, J = 9.6 Hz, 1H), 3.78 (dd, J = 12.3, 4.9 Hz, 1H), 3.64 (dd, J = 9.8, 8.2 Hz, 1H), 3.57−3.48 (m, 2H), 2.78−2.66 (m, 2H), 2.61 (ddd, J = 8.3, 6.4, 2.3 Hz, 2H), 2.05 (s, 3H).

^{13}C NMR (151 MHz, D_2O): δ = 178.36, 177.81, 177.47, 171.26, 135.79, 130.32, 81.47, 80.61, 77.22, 72.55, 65.90, 65.88, 63.57, 57.37, 33.19, 31.85, 25.07.

FAB−MS: m/z calcd for $C_{17}H_{27}N_2O_{10}$: 419.1666; found: 419.1667.

General Synthesis of Polymers (CEA-GlcNAc and AES-GlcNAc Polymers). An example of the polymerization procedure is shown in entries 1−6 in Table 1. CEA-GlcNAc (or AES-GlcNAc), DDMAT, and AIBN were added to DMSO.[26] The molar concentration of the monomer was set to 0.5 mol/L, and the molar ratio was [monomer]:[RAFT]:[initiator] = 1.25 × n:1:0.2 (n = 5, 10, and 20). The solution was then degassed by using freeze−pump−thaw cycles until no bubbles appeared. Next, it was allowed to react at 65 °C for 1.5−24 h under vacuum conditions. The mixture was then exposed to air and poured into 2-propanol to precipitate the polymeric product. The precipitate was purified through vigorous shaking twice in pure isopropyl alcohol and collected via suction filtration. The precipitate was dissolved in water, and the solution was dialyzed using a Spectra/Por 6 Dialysis Membrane Prewetting RC Tubing with a fractional molecular weight of 1000 D. After lyophilization, the product was obtained as a yellowish solid and stored at 4 °C.

The analytical data for poly(CEA-GlcNAc)$_{10}$ are as follows.

^{1}H NMR (600 MHz, D_2O): δ = 5.12 (s, 9H), 4.34 (brs, 21H), 3.99−3.74 (m, 29H), 3.67 (s, 10H), 3.55 (s, 19H), 2.69 (s, 20H), 2.40 (brs, 10H), 2.05 (s, 31H), 1.75 (br, 15H), 1.32 (brs, 18H), 1.25−1.13 (m, 6H), 0.92 (brt, J = 6.9 Hz, 3H).

^{13}C NMR (151 MHz, D_2O): δ = 177.04, 175.56, 81.22, 80.39, 77.06, 72.34, 63.79, 63.41, 57.25, 44.20, 37.45, 32.28, 25.07, 16.93.

The analytical data for poly(AES-GlcNAc)$_{10}$ are as follows.

^{1}H NMR (600 MHz, D_2O): δ = 5.09 (brd, J = 9.9 Hz, 9H), 4.35 (s, 35H), 3.95−3.82 (m, 17H), 3.78 (d, J = 10.4 Hz, 9H), 3.65 (brt, J = 8.7 Hz, 9H), 3.53 (s, 18H), 2.65 (m, 35H), 2.05

https://doi.org/10.1021/acsomega.5c02098
ACS Omega XXXX, XXX, XXX−XXX

(s, 31H), 1.77 (brs, 12H), 1.34 (brs, 18H), 1.23−1.13 (m, 6H), 0.94 (brs, 3H).

^{13}C NMR (151 MHz, D_2O): δ = 177.28, 176.80, 81.34, 80.42, 77.12, 72.40, 65.67, 63.45, 57.28, 44.12, 41.57, 32.97, 32.53, 31.57, 25.58, 25.07, 17.05.

The complete list is shown in the Supporting Information.

Synthesis of DBD-ED-Modified CDTPA. DBD-ED (186 mg, 0.652 mmol), CDTPA (244.86 mg, 0.607 mmol), and DMT-MM (185.9 mg, 0.672 mmol) were added to 30 mL of methanol (20 mM) at a molar ratio of 1:1:1 and stirred at 25 °C for 3 h. The mixture was then evaporated by using a rotary evaporator. The remaining sample was dispersed in water, and the precipitate was collected through filtration. The precipitate was dispersed in hexane and collected via filtration; this purification step was repeated twice. The collected precipitate was dried under a vacuum, and DBD-ED-CDTPA was obtained as an orangish solid (342 mg, 51.0 mmol, yield = 78.2%). The product was stored at −25 °C.

^{1}H NMR (400 MHz, DMSO-d_6): δ = 8.27 (s, 1H), 8.21 (d, J = 5.6 Hz, 1H), 7.83 (d, J = 8.2 Hz, 1H), 6.36 (d, J = 8.2 Hz, 1H), 3.46 (t, J = 6.5 Hz, 2H), 3.37 (t, J = 7.3 Hz, 4H), 2.70 (s, 6H), 2.46−2.24 (m, 4H), 1.84 (s, 3H), 1.70−1.58 (m, 2H), 1.24 (m, 20H), 0.85 (t, J = 6.9 Hz 3H).

^{13}C NMR (101 MHz, DMSO-d_6): δ = 218.33, 170.44, 146.41, 144.30, 141.36, 140.32, 119.12, 105.50, 98.73, 47.02, 42.54, 37.40, 36.41, 33.69, 31.23, 30.55, 28.93, 28.84, 28.73, 28.63, 28.34, 28.08, 27.22, 23.89, 22.03, 13.88.

FAB−MS: m/z calcd for $C_{29}H_{47}N_6O_4S_4$: 671.2542; found: 671.2536.

Synthesis of DBD-ED-CEA-GlcNAc Polymers. The DBD-ED-modified polymer was synthesized as described in the general polymerization procedure. Analytical data are listed in the Supporting Information.

Fast Atom Bombardment Mass Spectrometry (FAB−MS). FAB−MS was performed in the positive ion mode using a JEOL JMS-700 instrument with 3-nitrobenzylalcohol as the matrix in accordance with the manufacturer's instructions.

Matrix-Assisted Laser Desorption/Ionization Time-of-Flight Mass Spectrometry (MALDI-TOF−MS). MALDI-TOF−MS was performed in the positive linear mode using an Autoflex max (Bruker) equipped with a Smartbeam II laser. The polymer samples were mixed with a matrix (Super-DHB), spotted onto a MALDI plate, air-dried, and analyzed.

Gel Permeation Chromatography (GPC). GPC measurements were performed using an LC-91 × 0G NEXT instrument equipped with a JAIGEL-GS320 column (Japan Analytical Industry). A solution comprising 20% acetonitrile and 200 mM $NaNO_3$ was used at a flow rate of 5 mL/min at 25 °C. The molecular weights of the polymers were determined using a calibration curve based on pullulan standards (Shodex STANDARD P-82).

Cell Culture. 3LL and HeLa cells were maintained in high-glucose DMEM supplemented with 5% (v/v) fetal bovine serum (FBS) and 1% (v/v) antibiotics-antimycotics at 37 °C in a 5% CO_2 humidified incubator. MCF-7 cells were maintained in high-glucose MEM supplemented with 5% FBS, 1 mmol/L L-sodium pyruvate, 1% (v/v) insulin, and 1% (v/v) antibiotics-antimycotics at 37 °C in a 5% CO_2 humidified incubator. MCF10A cells were maintained in MEGM supplemented with 0.01% (v/v) cholera toxin and 1% (v/v) antibiotics-antimycotics at 37 °C in a 5% CO_2 humidified incubator. Vimentin-knockout (vim-KO) HeLa cells were produced by transfecting three human vimentin CRISPR/Cas9-knockout plasmids containing three types of vimentin-specific targeting guide RNA-coding sequences and vimentin homology-directed DNA repair plasmid that includes puromycin-resistance gene and red fluorescence protein gene (Santa Cruz Biotechnology, Dallas, TX, USA) into HeLa cells as described previously.[12] Vimentin gene-deleted and puromycin-resistance gene-integrated HeLa cells (vim-KO HeLa cells) were selected and established by culturing in DMEM/5% FBS/1% antibiotics-antimycotics containing 40 μg/mL puromycin to retain the transgene expression as a cell line. 3LL and MCF-7 cells were obtained from the Japanese Collection of Research Bioresources Cell Bank (Osaka, Japan), whereas HeLa cells were obtained from the RIKEN BRC CELL BANK (Tsukuba, Japan). MCF10A cells were obtained from the American Type Culture Collection (Manassas, VA, USA).

Flow Cytometry. Flow cytometry was performed using a Guava easyCyte instrument (Luminex). 3LL, HeLa, vim-KO HeLa, and MCF-7 cells were detached using accutase and suspended in DMEM. The cell suspension was incubated with DBD-ED-pCEA-GlcNAc 5 and 10 dissolved in phosphate-buffered saline (PBS) at 4 °C for 1 h. Next, the cells were washed twice with PBS and resuspended in PBS. MCF-7 cells were incubated with 2% antivimentin rod II domain antiserum or rabbit IgG (isotype control) in Hank's solution/10% FBS at 4 °C for 1 h. The cells were subsequently washed with PBS. They were then incubated in 0.2% (v/v) CF555 donkey antirabbit IgG (H + L) polyclonal antibody (secondary antibody) in HBSS containing 10% (v/v) FBS at 4 °C for 1 h. The cells were washed twice with PBS and resuspended in PBS. Furthermore, 40 and 80 μmol/L DBD-ED-pCEA-GlcNAc5 and 10 were incubated with 3LL cells at 4 °C for 2 h. Propidium iodide (PI) and FITC-annexin V staining for 3LL cells were conducted with an Annexin V-FITC apoptosis detection kit (Nacalai Tesque), according to the instructions.

Confocal Laser Scanning Microscopy. 3LL Cells (5×10^5 cells/mL) suspended in DMEM/5% FBS were cultured on 24 × 24 mm glass coverslips at 37 °C in a 5% CO_2 humidified incubator for 2 days. Next, they were incubated in 500 μg/mL DBD-ED-pCEA-GlcNAc 5 and 10 dissolved in Leibovitz's L15 medium at room temperature for 2 h. The cells were then washed with PBS and incubated with 2% (v/v) antivimentin rod II domain rabbit antiserum in HBSS containing 10% (v/v) FBS at room temperature for 1 h. The vimentin rod II domain is the cell surface-exposed domain of vimentin. Moreover, the antivimentin rod II domain antiserum can recognize cell surface-exposed vimentin. After 1 h of incubation, the cells were washed with PBS and incubated in 0.2% (v/v) CF555 donkey antirabbit IgG (H + L) secondary antibody in HBSS containing 10% (v/v) FBS at room temperature for 30 min. In the case of the internalization analysis for DBD-ED-pCEA-GlcNAc5, 3LL cells cultured on glass coverslips were incubated with 50 μg/mL DBD-ED-pCEA-GlcNAc5 for 1 h at 37 °C. At 1 h after incubation, the cells were then washed with PBS twice. Next, the cells were fixed with 4% (v/v) paraformaldehyde for 15 min and embedded in Fluoro-KEEPER Nonhardening Antifade Reagent with DAPI. They were subsequently observed under an A1R confocal laser scanning microscopy system (Nikon Solutions Co., Ltd., Tokyo, Japan) equipped with a Plan Apo 60 × A/1.40 Oil DIC H instrument (Nikon Solutions Co., Ltd.).

Preparation of Vimentin-Knockdown 3LL Cells by Transfecting Vimentin-siRNA. The transfection of vimen-

https://doi.org/10.1021/acsomega.5c02098
ACS Omega XXXX, XXX, XXX−XXX

Scheme 1. Synthetic Pathway of GlcNAc Polymers

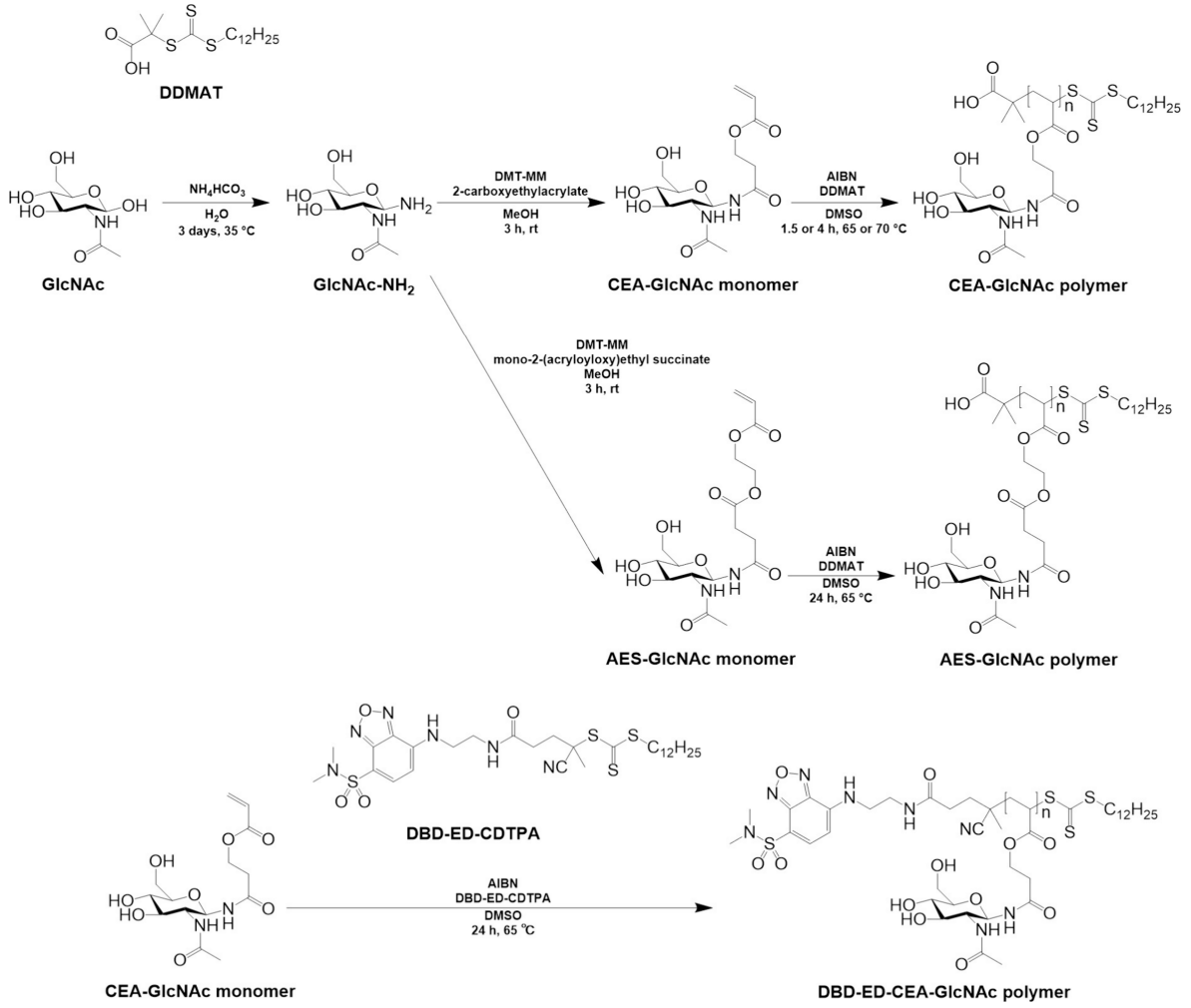

tin-siRNA into 3LL cells was transiently conducted using the reverse transfection method of the Lipofectamine RNAiMAX Transfection Reagent (Thermo Fisher), according to the instructions. The suspension of 3LL cells (3×10^4 cells/mL) was mixed with the Lipofectamine RNAiMAX Transfection Reagent (1 μL) and 6 pmol of vimentin-siRNA or negative-siRNA, and the mixture was cultured in 24-well plates at 37 °C in a 5% CO_2 humidified incubator for 3 days. As vimentin-siRNA, MISSION predesigned vimentin-siRNA (5′-gcgcaa-gauagauuuggaaua-3′) was purchased from Sigma-Aldrich. As a negative-siRNA, Silencer Select Negative Control No. 2 siRNA was purchased from Thermo Fisher. In 3 days of culture, the vimentin expression of 3LL cells transfected with vimentin-siRNA was confirmed to be decreased by Western blotting.

Western Blotting. 3LL cells (1×10^6 cells/mL) were cultured in 35 mm dishes containing 2 mL of DMEM/5% FBS for 1 day. In contrast, MCF-7 cells (1×10^6 cells/mL) were cultured in 35 mm dishes containing 2 mL of MEM/5% FBS for 4 days. After culture, the cells were incubated with serum-free DMEM or MEM containing 100 μg/mL pCEA- and pAES-GlcNAc 5, 10, and 20 for 1 day. Next, they were washed with PBS and lysed using a lysis buffer (1% (v/v) Triton X-100, 50 mM HEPES-NaOH (pH 7.5), 5 mM EDTA, 500 mM NaCl, 1% (v/v) protease inhibitor cocktail, and phosphatase inhibitor cocktail). The lysate was sonicated using a BRANSON Sonifier 250 (Emerson Electric Co., St. Louis, MO, USA) for 10 s under a 50% duty cycle (0.5 s cooling period). The insoluble matter was removed through centrifugation at 20,000×g for 10 min at 4 °C. The cell lysate was mixed at a 1:1 ratio with 2 × sample buffer (125 mmol/L Tris-HCl (pH 6.8), 4% (w/v) SDS, 10% (v/v) glycerol, 0.1% (w/v) bromophenol blue, and 200 mmol/L dithiothreitol) and heated at 95 °C for 5 min. The mixture was separated by using 12% SDS-PAGE, and the separated proteins were transferred onto Immobilon-P PVDF membranes. The membrane was blocked with Blocking One at room temperature for 10 min and subsequently incubated with a Signal Enhancer HIKARI solution containing approximately 0.1% (v/v) of each primary antibody at 4 °C for 1 day under gentle shaking. Next, the membrane was washed once with PBS containing Tween-20 (PBS-T) for 5 min and incubated with PBS-T containing 0.1% (v/v) HRP-conjugated donkey polyclonal antirabbit or mouse IgG secondary antibodies under gentle shaking. The membrane was then washed twice with PBS-T for 10 min each and incubated with the Immobilon Forte Western HRP substrate. Proteins were detected using a C−DiGit Blot Scanner (LI-COR Inc., Lincoln, NE, USA). The intensity of each protein band was quantified using ImageStudio Lite software (LI-COR). The relative value of each band and phosphor-Y705 STAT3 was normalized based on the band intensity for β-actin as a housekeeping gene and STAT3 corresponding to the band.

https://doi.org/10.1021/acsomega.5c02098
ACS Omega XXXX, XXX, XXX−XXX

Cell Viability. 3LL cells (2.5×10^5 cells/well) were cultured in a 48-well plate containing 250 μL of DMEM/5% FBS for 1 day. MCF-7 and MCF10A cells (2.0×10^4 cells/well) were cultured in a 48-well plate in 250 μL of MEGM for 6 days. After culture, the cells were incubated with serum-free DMEM or MEGM containing 50 and 100 μg/mL pCEA- and pAEC-GlcNAc 5, 10, and 20 for 1 day. Next, 5% (v/v) cell counting reagent SF (WST-8 assay) was added to each well. After 1 h of incubation, 100 μL of the medium from each well was transferred to each well of a 96-well plate. Absorbance was measured at 450 nm by using an iMark Microplate reader (Bio-Rad Laboratories, Inc., Hercules, CA, USA). Cell viability was assessed relative to the absorbance of a compound-free control.

Statistical Analysis. All experiments were independently performed 2−5 times. Statistical analyses were performed using GraphPad Prism 10.4 (GraphPad Software, Boston, MA, USA). Significance was determined using an unpaired ordinary one-way analysis of variance (ANOVA). Data are expressed as mean ± standard deviation.

RESULTS AND DISCUSSION

Synthesis of GlcNAc-Bearing Polymers for Suppressing Survivin Expression in 3LL Cancer Cells. We synthesized six types of GlcNAc-bearing polymers using RAFT polymerization to suppress the survivin expression in 3LL cells. We further synthesized two types of fluorescence-labeled GlcNAc-bearing polymers (DBD-ED-pCEA-GlcNAc5 and 10) to determine whether GlcNAc-bearing polymers can interact with 3LL cells via cell surface vimentin. Two types of monomers (CEA-GlcNAc and AES-GlcNAc) with different lengths between the main chain and the GlcNAc moiety were prepared to investigate the optimal side chain length for interacting with cells (Scheme 1). These monomers were polymerized with DDMAT or DBD-ED-CDTPA as RAFT agents to prepare three types of GlcNAc-bearing polymers of different sizes. The monomers, RAFT agents, and AIBN initiator were dissolved in DMSO with stoichiometries of [Monomer]:[RAFT reagents]:[Initiator] = 25:1:0.2, 12.5:1:0.2, and 6.25:1:0.2. They were then polymerized at 65 °C (only pCEA-GlcNAc20 was polymerized at 70 °C). Three different main lengths for pCEA-GlcNAc and pAES-GlcNAc polymers were obtained at a degree of polymerization of 4−22 (Scheme 1, Figure 1, and Table 1).

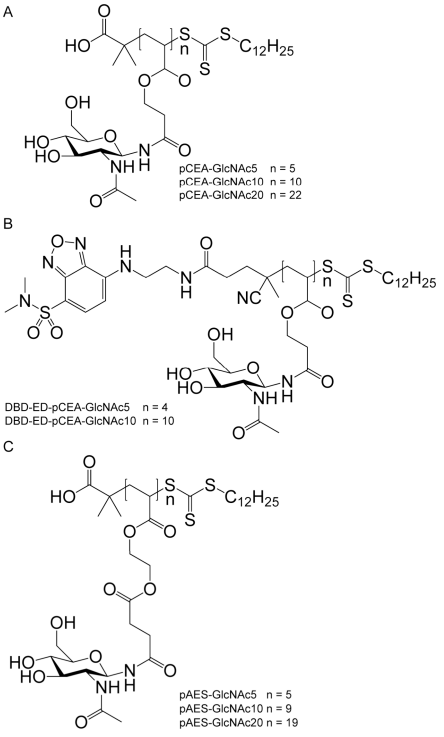

Figure 1. Structures of pCEA-GlcNAc (A), DBD-ED-pCEA-GlcNAc (B), and pAES-GlcNAc (C) polymers.

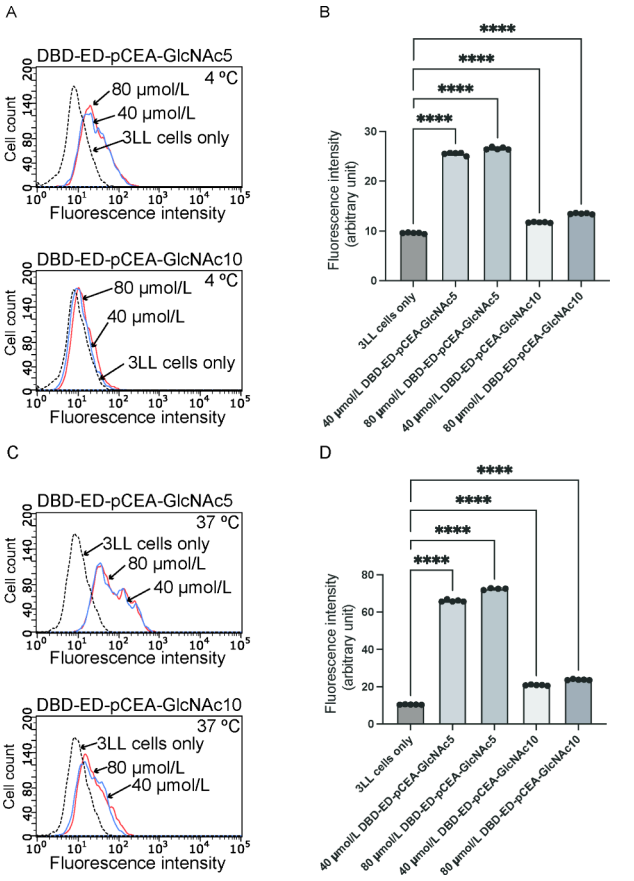

Figure 2. Flow cytometric analysis for the interaction of DBD-ED-pCEA-GlcNAc 5 and 10 with 3LL cells. (A) Flow cytometric analysis for the interaction of 40 and 80 μmol/L DBD-ED-pCEA-GlcNAc 5 and 10 with 3LL cells at 4 °C. (B) Mean fluorescence intensity of the interactions between these polymers and 3LL cells at 4 °C. (C) Flow cytometric analysis for the interaction of 40 μmol/L and 80 μmol/L DBD-ED-pCEA-GlcNAc 5 and 10 with 3LL cells at 37 °C. (D) Mean fluorescent intensity of the interactions between these polymers and 3LL cells at 37 °C. Statistical analyses were performed using one-way ANOVA (mean ± SD, n = 4−5, **** $p < 0.0001$).

Interaction between 3LL Cells and GlcNAc-Bearing Polymers via Cell Surface Vimentin. Confocal laser scanning microscopy and flow cytometry were used to determine whether the GlcNAc-bearing polymers DBD-ED-pCEA-GlcNAc5 and DBD-ED-pCEA-GlcNAc10 could interact with 3LL cells via cell surface vimentin. DBD-ED-pCEA-GlcNAc5 interacted with 3LL cells in a concentration-dependent manner, whereas DBD-ED-pCEA-GlcNAc10 showed minimal interaction with the cells regardless of concentration (Figure 2A). Furthermore, the fluorescence intensity revealed that a shorter pCEA-GlcNAc chain

https://doi.org/10.1021/acsomega.5c02098
ACS Omega XXXX, XXX, XXX−XXX

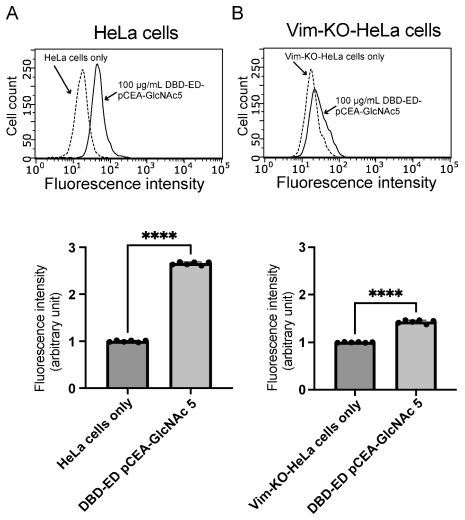

Figure 3. Flow cytometric analysis for the interaction of DBD-ED-pCEA-GlcNAc5 with HeLa and vimentin-knockout HeLa cells. (A) Flow cytometric analysis for the interactions of HeLa cells with 100 μg/mL DBD-ED-pCEA-GlcNAc5, and the mean fluorescence intensity of the interactions. (B) Flowcytometric analysis for the interactions of vimentin-knockout (Vim-KO)-HeLa cells with 100 μg/mL DBD-ED-pCEA-GlcNAc5, and the mean fluorescence intensity of the interactions. Statistical analyses were performed using one-way ANOVA (n = 3, **** $p < 0.0001$). Data are expressed as the mean ± SD.

improved cellular interaction (Figure 2B). Incubation at 4 °C inhibited the internalization of cell surface proteins. Therefore, the interaction between DBD-ED-pCEA-GlcNAc and 3LL cells was limited to the cell surface. Although DBD-ED-pCEA-GlcNAc10 showed insufficient interaction with 3LL cells, DBD-ED-pCEA-GlcNAc5 interacted efficiently owing to its shorter chain length. DBD-ED-pCEA-GlcNAc was assumed to be internalized intracellularly after incubation at 37 °C. This indicated that DBD-ED-pCEA-GlcNAc exhibited a stronger interaction with 3LL cells incubated at 37 °C than with those incubated at 4 °C (Figure 2C,D). Moreover, to confirm that the interactions of DBD-ED-pCEA-GlcNAc with 3LL cells were not a nonspecific interaction of some dead cells induced by the cytotoxicity of these polymers, the interaction of the fraction of living cells with DBD-ED-pCEA-GlcNAc5 in which the dead cells stained with PI were eliminated was examined at 37 °C by flow cytometry. The dead cells stained with PI in the cells reacted with DBD-ED-pCEA-GlcNAc5 and the control cells were approximately 18 and 14%, respectively, and the rate of dead cells between the cells added with DBD-ED-pCEA-GlcNAc5 and the control is almost the same. Therefore, it is considered that the acute cytotoxicity of DBD-ED-pCEA-GlcNAc5 is not high for at least 1 h after the addition. We observed that a fraction of living cells interacted with DBD-ED-pCEA-GlcNAc5 (Figure S37). This result demonstrates that the interaction of DBD-ED-pCEA-GlcNAc5 with 3LL cells is not a nonspecific interaction based on the dead cells.

We further investigated the interaction of DBD-ED-pCEA-GlcNAc5 with HeLa cells (high vimentin-expressing cells) and Vim-KO HeLa cells using flow cytometry to confirm whether this interaction depends on vimentin expression at 37 °C. DBD-ED-pCEA-GlcNAc5 interacted with HeLa cells but not with Vim-KO HeLa cells (Figure 3). Vim-KO HeLa cells do not express vimentin completely because the vimentin gene was eliminated by the CRISPR/Cas9 genome editing technique.[12] Moreover, in these cells, the puromycin-resistance gene has been integrated into the vimentin gene-deleted site alternatively. Therefore, since the vimentin-expressing cells in the population of vim-KO-HeLa cells cannot survive in the presence of puromycin, we completely selected and established vim-KO-HeLa cells that do not express vimentin protein by treating them with puromycin as a cell line. We had previously reported that vim-KO-HeLa cells selected by adding puromycin cannot express vimentin by Western blotting.[12]

These results suggest that DBD-ED-pCEA-GlcNAc5 interacts with HeLa cells via vimentin on the cell surface. Thus, we used confocal laser scanning microscopy and immunocytochemistry to investigate whether DBD-ED-pCEA-GlcNAc5 interacted with 3LL cells by binding to the cell surface vimentin. As shown in Figure 4, vimentin-stained areas were localized to the surface of 3LL cells. DBD-ED-pCEA-GlcNAc5-stained regions were observed on the 3LL cell surface. The vimentin-immunostained and DBD-ED-pCEA-GlcNAc-stained areas were colocalized to the surface of 3LL cells (Figure 4A). DBD-ED-pCEA-GlcNAc5 was incubated with 3LL cells for 1 h at 37 °C. The staining regions of DBD-ED-pCEA-GlcNAc5 were observed in the intercellular zone of the 3LL cells (Figure 4B). Therefore, the internalization of DBD-ED-pCEA-GlcNAc5 into 3LL cells was demonstrated by incubating at 37 °C for 1 h. These results suggest that DBD-ED-pCEA5 was internalized into 3LL cells via cell surface vimentin.

Modulation of Survivin Expression through the Addition of Various GlcNAc-Bearing Polymers in 3LL Cells. In our previous study, the interaction of GlcNAc-bearing polymers with cell surface vimentin suppressed survivin expression in NHDF.[13] Therefore, we investigated whether our GlcNAc-bearing polymers could suppress survivin expression in 3LL cells. Western blot analysis of 3LL cells indicated that pCEA- and pAES-GlcNAc5 suppressed survivin expression more strongly than pCEA- and pAES-GlcNAc10 and 20 (Figure 5). Each value of survivin expression was indicated by normalizing the β-actin expression. Since living cells constantly express β-actin as a housekeeping gene, the value of survivin expression normalized by the β-actin expression demonstrates the survivin expression in living cells. We previously reported that GlcNAc-bearing polymers upregulate the expression of p53 and downregulate that of STAT3 phosphorylation in NHDF.[13] In addition, persistent activation of STAT3 induces survivin expression in various cancer cells.[27] Therefore, we evaluated the expression of p53 and the phosphorylation of STAT3 in pCEA- and pAES-GlcNAc-treated 3LL cells. p53 expression was upregulated, whereas STAT3 phosphorylation was downregulated in these cells (Figure 5). Upregulation of p53 expression suppresses the phosphorylation of STAT3.[28] Thus, our findings suggest that pCEA- and pAES-GlcNAc increase the p53 expression levels. Moreover, upregulation of p53 expression suppresses persistently activated STAT3, and the inactivation of STAT3 suppresses survivin expression. To confirm whether the suppression of survivin expression by pCEA- and pAES-GlcNAc was induced by the interaction with cell surface vimentin, we examined the survivin expression in vimentin-knockdown 3LL cells treated with 100 μg/mL pCEA-GlcNAc5. Vimentin-knockdown 3LL cells were produced by transfecting the vimentin-siRNA for 72 h. Vimentin expression in 3LL cells treated with vimentin-siRNA for 72h was

https://doi.org/10.1021/acsomega.5c02098
ACS Omega XXXX, XXX, XXX−XXX

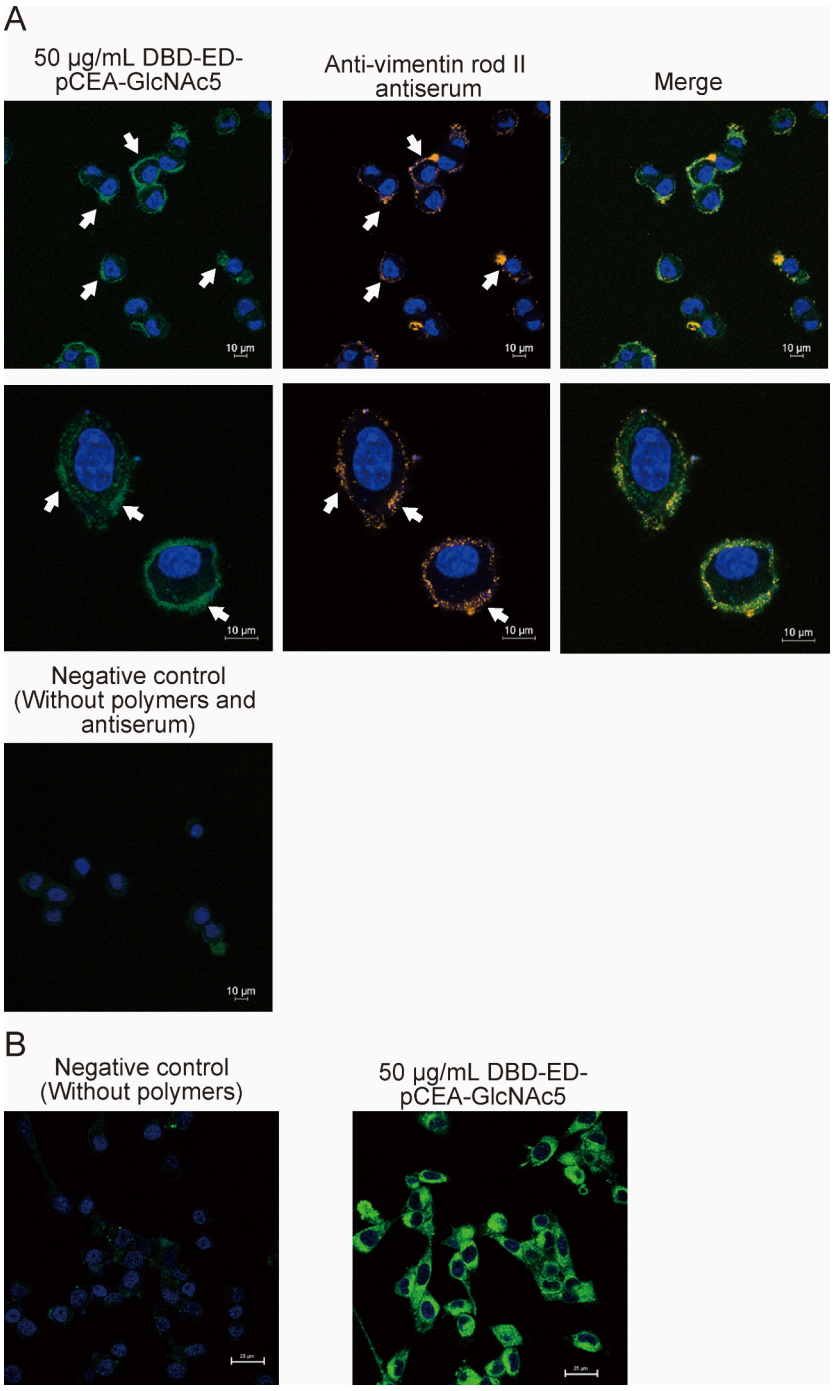

Figure 4. Confocal laser scanning microscopy for the interaction of 3LL cells with DBD-ED-pCEA-GlcNAc5 through cell surface vimentin. (A) Immunostaining images of antivimentin rod II antibody showing cell surface vimentin (orange) in 3LL cells, DBD-ED-pCEA-GlcNAc 5-staining images (green), and merged images of cell surface vimentin-immunostaining and DBD-ED-pCEA-GlcNAc 5-staining (upper panels). The lower panels show magnified images, and the arrows indicate the colocalized area between the immunostained and DBD-ED-pCEA-GlcNAc 5-stained regions. Negative control indicates the only immunostaining with the rabbit normal antiserum and the secondary antibody. (B) Internalization of the image for DBD-ED-pCEA-GlcNAc5 in 3LL cells. After 3LL cells were incubated with 50 μg/mL DBD-ED-pCEA-GlcNAc5 for 1 h at 37 °C, the staining regions of DBD-ED-pCEA-GlcNAc5 (green) were observed in intercellular zones by confocal laser scanning microscopy. Negative control is only DAPI staining. The cell nucleus was stained with DAPI (blue). Scale bars are 10 μm.

confirmed to be reduced (Figure 6A). At 72 h after the transfection of negative- or vimentin-siRNA to 3LL cells, each 3LL cell was incubated with 100 μg/mL pCEA-GlcNAc5 for 1 h. At 24 h after incubation for 1 h, survivin expression was detected by Western blotting. Since Figure 4B demonstrates that pCEA-GlcNAc5 was incorporated into the intracellular region for 1 h, it is considered that the 1 h of incubation with pCEA-GlcNAc5 was adequate for the stimulation. Survivin expression in negative-siRNA-treated cells was downregulated by treatment with pCEA-GlcNAc5, whereas that in vimentin-siRNA-treated cells was not (Figure 6B). These results demonstrated that pCEA-GlcNAc5 was incorporated intracellularly through cell surface vimentin and downregulated survivin expression.

https://doi.org/10.1021/acsomega.5c02098
ACS Omega XXXX, XXX, XXX−XXX

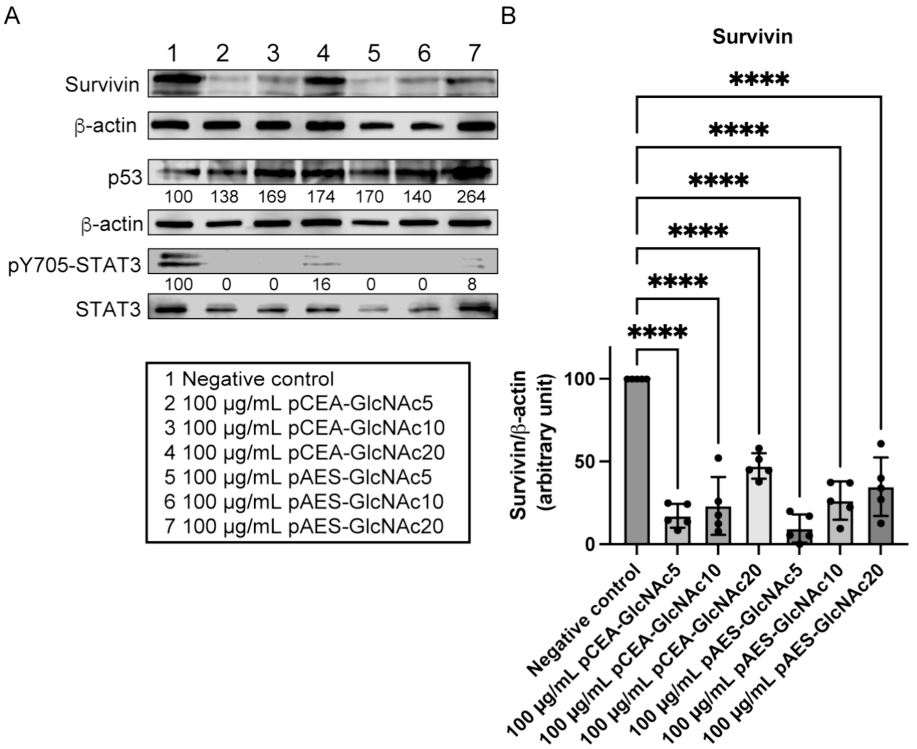

Figure 5. Expression of survivin, p53, and phosphorylated STAT3 in pCEA- and pAES-GlcNAc5-, 10-, and 20-stimulated 3LL cells, as determined using Western blotting. (A) Expression and phosphorylation levels of various proteins in 3LL cells 24 h after the addition of 100 μg/mL pCEA- and pAES-GlcNAc5, 10, and 20. The numbers under the bands or the bands for phosphorylated proteins indicate the relative values of each band normalized based on the density of the band for β-actin or unphosphorylated proteins corresponding to the band, respectively. Cropped images for Western blots are representative blots from 2−5 independent experiments. (B) Survivin expression levels in pCEA- and pAES-GlcNAc5-, 10-, and 20-stimulated 3LL cells. Values are based on the intensity of each survivin band relative to the corresponding β-actin band (mean ± SD). Statistical analyses were performed using one-way ANOVA (n = 5, **** $p < 0.0001$).

Antitumor Effects of pCEA- and pAES-GlcNAc in 3LL. Treatment with pCEA and pAES-GlcNAc suppressed survivin expression. Survivin is involved in resistance to apoptosis and cell-cycle progression.[1] Therefore, we investigated the viability of 3LL cells following treatment with 50 and 100 μg/mL pCEA- and pAES-GlcNAc. The viability of these cells significantly decreased (Figure 7). Addition of pCEA- and pAES-GlcNAc5 to 3LL cells decreased the cell viability more strongly than that of pCEA- and pAES-GlcNAc10 or 20. These results suggest that the suppression of survivin and upregulation of p53 expression through treatment with pCEA- and pAES-GlcNAc could induce cell death in cancer cells. Since the cell death induced by treatment with pCEA- and pAES-GlcNAc was caused by the suppression of survivin, the cell death is considered to be apoptosis. Therefore, the staining of FITC-annexin V was conducted for 3LL cells treated with 100 μg/mL pCEA-GlcNAc5 for 24 h, and the staining was evaluated by flow cytometry. Although normal 3LL cells were slightly and nonspecifically stained by FITC-annexin V, 3LL cells treated with 100 μg/mL pCEA-GlcNAc5 for 24 h were stained more strongly than normal 3LL cells (Figure S40). Therefore, the cell death of 3LL cells treated with pCEA-GlcNAc5 was demonstrated to be apoptosis.

Survivin Expression through pCEA- and pAES-GlcNAc Addition in MCF-7 Cells. MCF-7 breast cancer cells express high levels of survivin. Therefore, we investigated whether survivin expression in these cells was downregulated following treatment with pCEA and pAES-GlcNAc5, 10, or 20. First, we used flow cytometry to investigate whether MCF-7 cells express cell surface vimentin and whether it binds to DBD-ED-pCEA-GlcNAc5 and 10. MCF-7 cells typically express cell surface vimentin.[18,29] Consistently, MCF-7 cells expressed cell surface vimentin and interacted with pCEA-GlcNAc5 and pCEA-GlcNAc10 in the present study (Figure 8). Moreover, survivin expression in these cells was downregulated by 100 μg/mL pCEA- and pAES-GlcNAc5 (Figure 9A). However, treatment with pCEA- and pAES-GlcNAc5, 10, or 20 did not decrease the viability of these cells (Figure 9B). In contrast, the viability of 3LL cells treated with pCEA- and pAES-GlcNAc polymers decreased (Figure 7). The doubling time of MCF-7 cells is 52−60 h, and that of the 3LL cells is approximately 33 h. Therefore, the proliferative rate of MCF-7 cells is lower than that of 3LL cells. Survivin expression is controlled through a progression of the cell cycle and is observed only in the G2−M phase. This protein interacts with the tubulin of the mitotic spindle in the M phase, and the interaction is involved in the regulation of mitosis.[1−6] Thus, we hypothesized that the 24 h decline in survivin expression in MCF-7 cells could not affect their viability because the progression of the cell cycle for MCF-7 cells is slow. We examined the viability of MCF-7 cells treated with pCEA-GlcNAc5 and 10 for 96 h. The decrease in the viability of these MCF-7 cells was observed at 96 h (Figure 9B). Next, as nontumorigenic and immortalized human breast epithelial cells corresponding to MCF-7 cells, breast cancer cells, we investigated whether these polymers could affect the viability of MCF10A cells.[30] MCF10A cells hardly express survivin, and the doubling time is approximately 16 h.[31] Their viability was not decreased by treatment with 100 μg/mL

https://doi.org/10.1021/acsomega.5c02098
ACS Omega XXXX, XXX, XXX−XXX

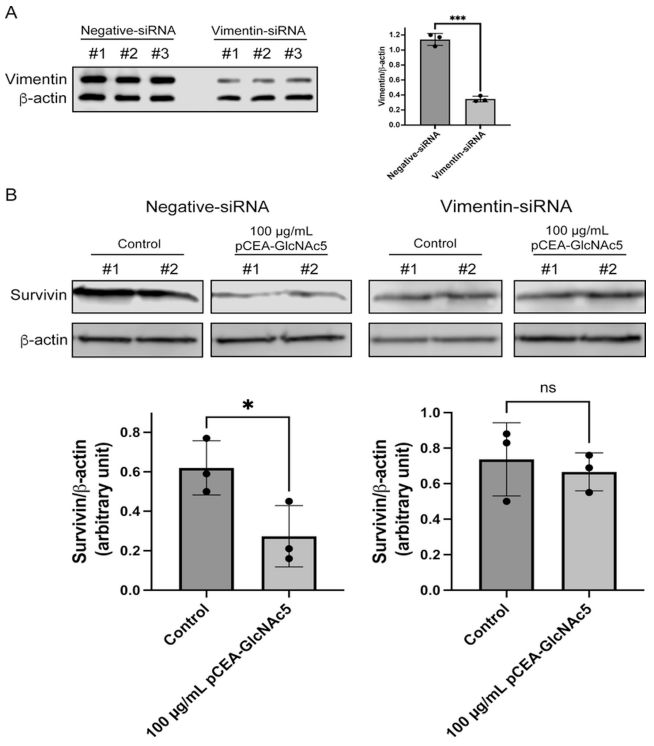

Figure 6. Expression of survivin in negative- and vimentin-siRNA-treated 3LL cells treated with 100 μg/mL pCEA-GlcNAc5. (A) Expression of vimentin in negative- and vimentin-siRNA-treated 3LL cells. (B) Survivin expression levels in negative- and vimentin-siRNA-treated 3LL cells by treating with 100 μg/mL pCEA-GlcNAc5. Values are based on the intensity of each vimentin or survivin band relative to the corresponding β-actin band (mean ± SD). Statistical analyses were performed using Welch's t test (n = 3, * p < 0.05, *** p < 0.001).

pCEA- and pAES-GlcNAc5, 10, and 20 in the present study (Figure 9C). These results suggest that these polymers affect survivin-expressing tumorigenic cells and do not affect nontumorigenic cells, such as MCF10A cells.

In this study, pCEA and pAES-GlcNAc5 strongly suppressed survivin expression and induced apoptosis in the 3LL cells. This suppression was thought to depend on the interaction of these polymers with the 3LL cells. The interaction of carbohydrates with lectins is typically augmented by increasing carbohydrate ligands; this phenomenon is called the "cluster effect."[23,32] In the present study, the shortest polymer (pCEA-GlcNAc5 with five GlcNAc ligands) interacted with HeLa and 3LL cells more strongly than pCEA-GlcNAc10, which has 10 GlcNAc ligands. However, the addition of GlcNAc monosaccharides to 3LL cells did not reduce survivin expression (Figure S38). Moreover, GlcNAc monosaccharides could not interact with cell surface vimentin-expressing cells in our previous studies.[11−13] These findings demonstrate that approximately five GlcNAc ligands but not GlcNAc monosaccharides may be adequate for carbohydrate recognition by vimentin.

Numerous glycans are present on the cell surface, and the pericellular space is hydrophilic. Moreover, cell surface vimentin may be slightly exposed to the cellular surface membrane because vimentin is not a general receptor protein on the cell surface. Long GlcNAc-bearing polymers and GlcNAc monosaccharides are presumed to not be readily accessible to superficial cell membrane-exposed cell surface vimentin because of their high hydrophilicity. This is attributed to the repulsion of the cell surface glycans. In addition, the hydrophobicity of polymers may facilitate close access of GlcNAc-bearing polymers to cellular surface membranes.[33] Because pCEA- and pAES-GlcNAc5 have a dodecyl alkyl chain derived from the DDMAT and RAFT agents, the dodecyl alkyl chain site attracts GlcNAc moieties to the cell membrane-exposed cell surface vimentin. In this study, the minimum number of GlcNAc ligands required to bind to these cells could not be determined because water-soluble GlcNAc polymers that consist of less than five GlcNAc ligands were not prepared. Therefore, conjugation of the hydrophobic moiety, which possesses some water solubility, to minimal GlcNAc ligand-bearing materials is important for achieving strong interactions with cell surface vimentin.

Survivin expression is regulated by the STAT3 pathway, and STAT3 is constitutively activated in many cancer cells. The activation and phosphorylation of STAT3 are suppressed by p53 expression.[34] The addition of CEA and pAES-GlcNAc to 3LL cells induced p53 expression, which consequently downregulated STAT3 phosphorylation. This resulted in a decreased survivin expression. The interaction of GlcNAc-bearing polymers with cell surface vimentin stimulated phosphorylated p38MAPK, which subsequently increased p53 levels in our previous study.[35] These findings suggest that the downregulation of survivin expression based on pCEA- and pAES-GlcNAc can only be performed in p53-expressing cancer cells, such as 3LL and MCF-7 cells. Survivin is highly expressed in drug-resistant cancer cells such as stem cells. Thus, combining anticancer drugs such as doxorubicin with pCEA- and pAES-GlcNAc5 may effectively kill wild-type p53-expressing cancer cells. Given the selective targeting of cancer cells by pCEA- and pAES-GlcNAc5 through binding to cell surface vimentin, these polymers hold significant potential for developing targeted drug delivery systems. Specifically, conjugating an anticancer drug to pCEA- or pAES-GlcNAc5 could facilitate the effective delivery of the therapeutic agent to cancer tissues. However, these polymers did not downregulate survivin expression in MDA-MB-231 cells (Figure S39). The p53 of MDA-MB-231 cells is mutated.[36] Moreover, since the p53 protein in HeLa cells was inactivated by the human papillomavirus-E6 protein, it is presumed that these polymers cannot downregulate survivin expression in HeLa cells.[37] Thus, our approach has some limitations. The downregulation of survivin expression by GlcNAc-bearing polymers may have been limited to cancer cells lacking a mutated p53 and highly activating STAT3 in the present study. Because survivin expression is regulated through various pathways, our approach may not be effective for cancer cells that express survivin through pathways other than the STAT3 pathway.[5]

CONCLUSIONS

This study demonstrates the potential application of GlcNAc-modified polymers, specifically pCEA- and pAES-GlcNAc5, as novel anticancer therapeutics that suppress survivin expression. Although previous studies have explored various therapeutic approaches for the suppression of survivin expression,[22] these approaches often lack selectivity for cancer cells, consequently raising concerns about potential side effects on healthy tissues. Our therapeutic approach leverages the selective targeting of cell surface vimentin, a receptor frequently overexpressed in cancer cells, including stem cells and drug-resistant cells. This selective targeting strategy offers a promising avenue for the

https://doi.org/10.1021/acsomega.5c02098
ACS Omega XXXX, XXX, XXX−XXX

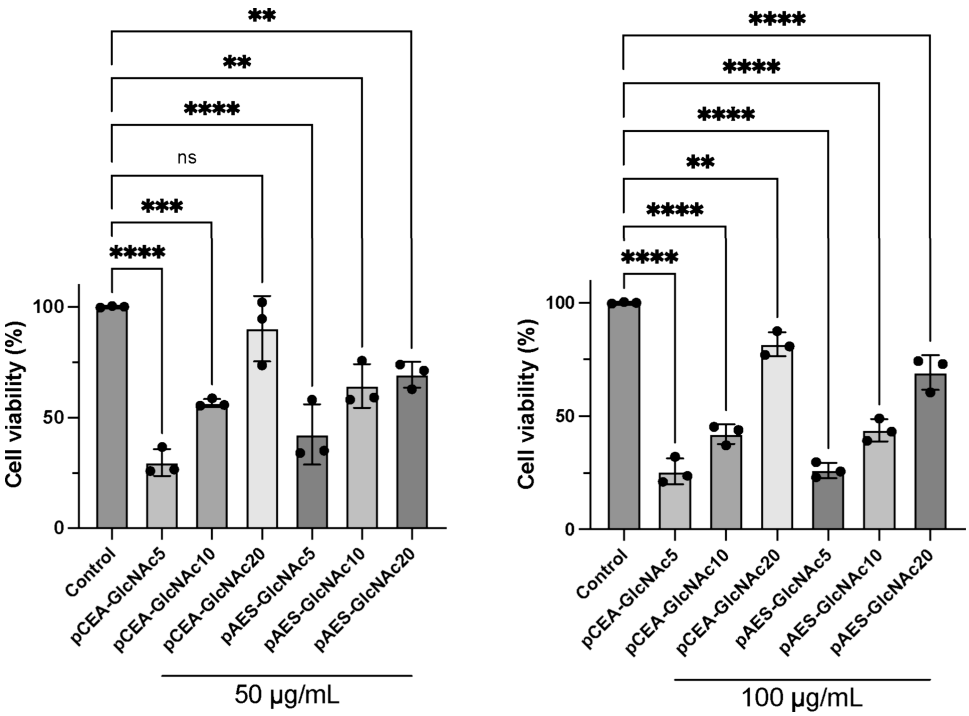

Figure 7. Viability of pCEA- and pAES-GlcNAc5-, 10-, and 20-stimulated 3LL. The viability of 3LL cells was measured using the WST-8 assay 24 h after adding these polymers. The left and right panels indicate 50 and 100 μg/mL of these polymers, respectively. Statistical analyses were performed using one-way ANOVA (n = 3−6; ns, nonsignificant; ** $p < 0.01$, *** $p < 0.001$, **** $p < 0.0001$). Data are expressed as the mean ± SD.

development of novel anticancer therapies with improved safety profiles.

■ ASSOCIATED CONTENT

Supporting Information

The Supporting Information is available free of charge at https://pubs.acs.org/doi/10.1021/acsomega.5c02098.

Additional methodological details and Figures S1−S38 (PDF)

■ AUTHOR INFORMATION

Corresponding Authors

Shingo Kobayashi − *Institute for Materials Chemistry and Engineering, Kyushu University, Fukuoka 819-0395, Japan;* Present Address: Department of Pharmacokinetics and Biopharmaceutics, Institute of Biomedical Sciences, Tokushima University, 1-78-1 Sho-machi, Tokushima 770-8501, Japan; orcid.org/0000-0002-8357-8654; Email: shingo_kobayashi@ms.ifoc.kyushu-u.ac.jp, kobayashi.shingo@tokushima-u.ac.jp

Hirohiko Ise − *Institute for Materials Chemistry and Engineering, Kyushu University, Fukuoka 819-0395, Japan;* orcid.org/0000-0002-4948-9375; Email: ise@ms.ifoc.kyushu-u.ac.jp

Authors

Karera Kitagawa − *Applied Chemistry, Graduate School of Engineering, Kyushu University, Fukuoka 819-0395, Japan*

Yoshiko Miura − *Chemical Engineering, Graduate School of Engineering, Kyushu University, Fukuoka 819-0395, Japan;* orcid.org/0000-0001-8590-6079

Masaru Tanaka − *Institute for Materials Chemistry and Engineering, Kyushu University, Fukuoka 819-0395, Japan;* orcid.org/0000-0002-1115-2080

Complete contact information is available at: https://pubs.acs.org/10.1021/acsomega.5c02098

Author Contributions

Conceptualization, writing—original draft preparation, writing—review and editing: K.K., S.K., and H.I.; project administration and funding acquisition: S.K. and H.I.; methodology: K.K., S.K., and H.I.; validation, formal analysis, and investigation: K.K., S.K., and H.I.; supervision: Y.M., M.T., S.K., and H.I.. All of the authors have given approval to the final version of the manuscript.

Funding

This work was supported by JSPS KAKENHI (grant number JP 22K12818) and the Cooperative Research Program of the Network Joint Research Center for Materials and Devices.

Notes

The authors declare no competing financial interest.

■ ACKNOWLEDGMENTS

The authors thank the SOMAR CORPORATION for providing financial support. The authors also thank Dr. Satoru Kidoaki and Ms. Yukie Tsuji for lending the devices and for their technical advice. The authors would like to thank Editage (www.editage.jp) for English language editing.

■ ABBREVIATIONS

GlcNAc,*N*-acetylglucosamine; CEA,2-carboxyethyl acrylate; AES,mono(2-acryloyloxyethyl) succinate

https://doi.org/10.1021/acsomega.5c02098
ACS Omega XXXX, XXX, XXX−XXX

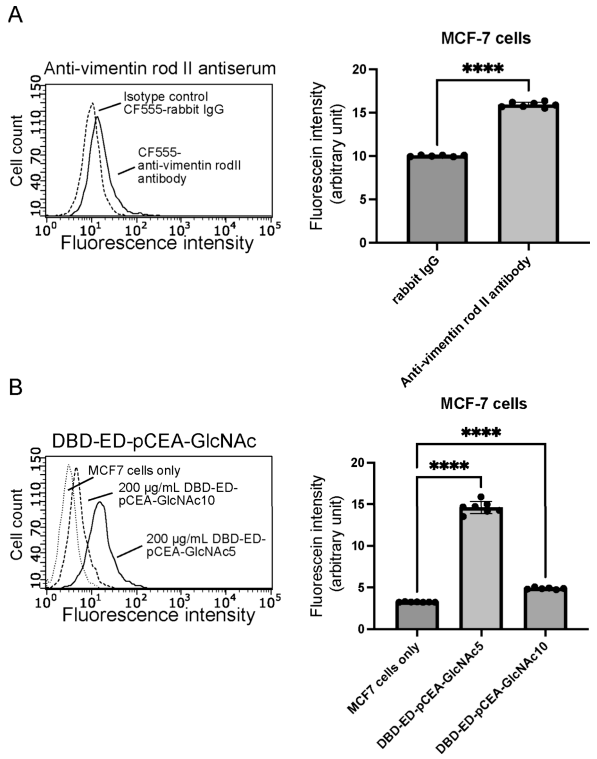

Figure 8. Flow cytometric analysis for the interaction of 2% (v/v) antivimentin rod II domain rabbit antiserum and 200 μg/mL pCEA-GlcNAc 5 with MCF-7 cells. (A) Flow cytometric analysis for the interaction of 2% (v/v) antivimentin rod II domain rabbit antiserum with MCF-7 cells. (B) Mean fluorescence intensity of the interactions between 200 μg/mL pCEA-GlcNAc 5 and MCF-7 cells. Statistical analyses were performed using one-way ANOVA (mean ± SD, $n = 6$, **** $p < 0.0001$).

REFERENCES

(1) Wheatley, S. P.; Altieri, D. C. Survivin at a glance. *J. Cell. Sci.* **2019**, *132*, jcs223826.

(2) Siragusa, G.; Tomasello, L.; Giordano, C.; Pizzolanti, G. Survivin (BIRC5): Implications in cancer therapy. *Life. Sci.* **2024**, *350*, No. 122788.

(3) Li, F.; Aljahdali, I.; Ling, X. Cancer therapeutics using survivin BIRC5 as a target: what can we do after over two decades of study? *J. Exp. Clin. Cancer. Res.* **2019**, *38*, 368.

(4) Kondapuram, S. K.; Ramachandran, H. K.; Arya, H.; Coumar, M. S. Targeting survivin for cancer therapy: Strategies, small molecule inhibitors and vaccine based therapeutics in development. *Life. Sci.* **2023**, *335*, No. 122260.

(5) Martínez-García, D.; Manero-Rupérez, N.; Quesada, R.; Korrodi-Gregório, L.; Soto-Cerrato, V. Therapeutic strategies involving survivin inhibition in cancer. *Med. Res. Rev.* **2019**, *39*, 887−909.

(6) Fang, X. L.; Cao, X. P.; Xiao, J.; Hu, Y.; Chen, M.; Raza, H. K.; Wang, H. Y.; He, X.; Gu, J. F.; Zhang, K. J. Overview of role of survivin in cancer: expression, regulation, functions, and its potential as a therapeutic target. *J. Drug. Target.* **2024**, *32*, 223−240.

(7) Wang, Q.; Greene, M. I. Survivin as a Therapeutic Target for the Treatment of Human Cancer. *Cancers (Basel).* **2024**, *16* (9), No. 1705.

(8) Pachimatla, A. G.; Fenstermaker, R.; Ciesielski, M.; Yendamuri, S. Survivin in lung cancer: a potential target for therapy and prevention-a narrative review. *Transl. Lung. Cancer. Res.* **2024**, *13*, 362−374.

(9) Kita, A.; Nakahara, T.; Takeuchi, M.; Kinoyama, I.; Yamanaka, K.; Minematsu, T.; Mitsuoka, K.; Fushiki, H.; Miyoshi, S.; Sasamata, M.; Miyata, K. Survivin supressant: a promising target for cancer therapy and pharmacological profiles of YM155. *Folica Pharmacol. Jpn.* **2010**, *136* (4), 198−203.

(10) Tolcher, A. W.; Quinn, D. I.; Ferrari, A.; Ahmann, F.; Giaccone, G.; Drake, T.; Keating, A.; Bono, J. S. A phase II study of YM155, a novel small-molecule suppressor of survivin, in castration-resistant taxane-pretreated prostate cancer. *Ann. Oncol.* **2012**, *23* (4), 968−973.

(11) Ise, H.; Kobayashi, S.; Goto, M.; Sato, T.; Kawakubo, M.; Takahashi, M.; Ikeda, U.; Akaike, T. Vimentin and desmin possess GlcNAc-binding lectin-like properties on cell surfaces. *Glycobiology* **2010**, *20* (7), 843−864.

(12) Ise, H.; Yamasaki, S.; Sueyoshi, K.; Miura, Y. Elucidation of GlcNAc-binding properties of type III intermediate filament proteins, using GlcNAc-bearing polymers. *Genes Cells* **2017**, *22* (10), 900−917.

(13) Ise, H.; Araki, Y.; Song, I.; Akatsuka, G. N-acetylglucosamine-bearing polymers mimicking O-GlcNAc-modified proteins elicit anti-fibrotic activities in myofibroblasts and activated stellate cells. *Glycobiology* **2023**, *33* (1), 17−37.

(14) Ise, H.; Matsunaga, K.; Shinohara, M.; Sakai, Y. Improved Isolation of Mesenchymal Stem Cells Based on Interactions between *N*-Acetylglucosamine-Bearing Polymers and Cell-Surface Vimentin. *Stem Cells Int.* **2019**, *2019* (1), No. 4341286.

(15) Song, I.; Ise, H. Development of a Gene Delivery System of Oligonucleotides for Fibroses by Targeting Cell-Surface Vimentin-Expressing Cells with N-Acetylglucosamine-Bearing Polymer-Conjugated Polyethyleneimine. *Polymers* **2020**, *12* (7), No. 1508.

(16) Ise, H.; Goto, M.; Komura, K.; Akaike, T. Engulfment and clearance of apoptotic cells based on a GlcNAc-binding lectin-like property of surface vimentin. *Glycobiology* **2012**, *22* (6), 788−805.

(17) Ivaska, J.; Pallari, H. M.; Nevo, J.; Eriksson, J. E. Novel functions of vimentin in cell adhesion, migration, and signaling. *Exp. Cell Res.* **2007**, *313* (10), 2050−2062.

(18) Satelli, A.; Mitra, A.; Brownlee, Z.; Xia, X.; Bellister, S.; Overman, M. j.; Kopetz, S.; Ellis, L. M.; Meng, Q. H.; Li, S. Epithelial−Mesenchymal Transitioned Circulating Tumor Cells Capture for Detecting Tumor Progression. *Clin. Cancer Res.* **2015**, *21* (4), 899−906.

(19) Arentz, G.; Chataway, T.; Price, T. J.; Izwan, Z.; Hardi, G.; Cummins, A. G.; Hardingham, J. E. Desmin expression in colorectal cancer stroma correlates with advanced stage disease and marks angiogenic microvessels. *Clin. Proteomics* **2011**, *8* (1), 16.

(20) Satelli, A.; Li, S. Vimentin in cancer and its potential as a molecular target for cancer therapy. *Cell. Mol. Life Sci.* **2011**, *68*, 3033−3046.

(21) Hwang, B.; Ise, H. Multimeric conformation of type III intermediate filaments but not the filamentous conformation exhibits high affinity to lipid bilayers. *Genes Cells* **2020**, *25* (6), 413−426.

(22) Wang, Q.; Greene, M. I. Survivin as a Therapeutic Target for the Treatment of Human Cancer. *Cancers* **2024**, *16* (9), No. 1705.

(23) Zhou, C.; Reesink, H. L.; Putnam, D. A. Selective and Tunable Galectin Binding of Glycopolymers Synthesized by a Generalizable Conjugation Method. *Biomacromolecules* **2019**, *20* (10), 3704−3712.

(24) Likhosherstov, L. M.; Novikova, O. S.; Derevitskaja, V. A.; Kochetkov, N. K. A new simple synthesis of amino sugar β-D-glycosylamines. *Carbohydr. Res.* **1986**, *146* (1), C1−C5.

(25) Liu, F. C.; Su, C. R.; Wu, T. Y.; Su, S. G.; Yang, H. L.; Lin, J. H. Y.; Wu, T. S. Efficient ^{1}H-NMR Quantitation and Investigation of *N*-Acetyl-D-glucosamine (GlcNAc) and *N*,*N*′-Diacetylchitobiose $(GlcNAc)_2$ from Chitin. *Int. J. Mol. Sci.* **2011**, *12* (9), 5828−5843.

(26) Moad, G.; Rizzardo, E.; Thang, S. H. Living Radical Polymerization by the RAFT Process − A Second Update. *Aust. J. Chem.* **2009**, *62* (11), 1402−1472.

(27) Banerjee, K.; Resat, H. Constitutive activation of STAT3 in breast cancer cells: A review. *Int. J. Cancer* **2016**, *138* (11), 2570−2578.

(28) Güllülü, Ö.; Hehlgans, S.; Rödel, C.; Fokas, E.; Rödel, F. Tumor Suppressor Protein p53 and Inhibitor of Apoptosis Proteins in Colorectal Cancer-A Promising Signaling Network for Therapeutic Interventions. *Cancers* **2021**, *13* (4), No. 624.

https://doi.org/10.1021/acsomega.5c02098
ACS Omega XXXX, XXX, XXX−XXX

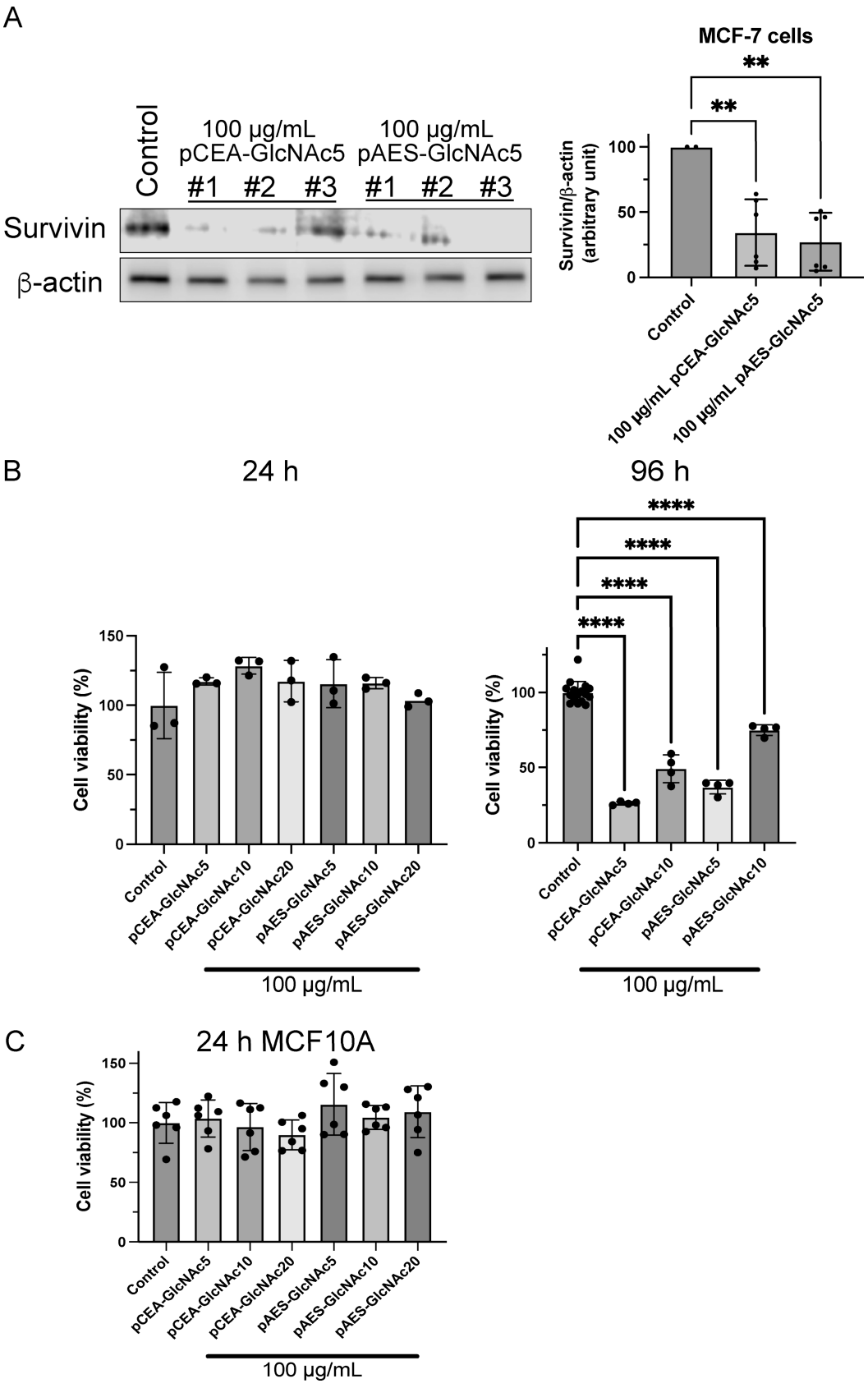

Figure 9. Expression of survivin in pCEA-GlcNAc5-stimulated MCF-7 cells, as determined using Western blotting; viability in pCEA- and pAES-GlcNAc5-, 10-, and 20-stimulated MCF-7 cells and MCF10A. (A) Survivin expression levels in MCF-7 cells 24 h after the addition of 100 μg/mL pCEA- and pAES-GlcNAc5. The graph indicates the relative values of each band normalized based on the density of the band for β-actin. Cropped images for Western blots are representative blots. (B) Viability of MCF-7 cells, as measured using the WST-8 assay 24 and 96 h after the addition of

https://doi.org/10.1021/acsomega.5c02098
ACS Omega XXXX, XXX, XXX−XXX

Figure 9. continued

100 μg/mL of these polymers (mean ± SD). (C) Viability of MCF10A cells, as measured using the WST-8 assay 24 h after adding 100 μg/mL of these polymers. Statistical analyses were performed using one-way ANOVA (n = 3−6, ** p < 0.01, **** p < 0.0001).

(29) Komura, K.; Ise, H.; Akaike, T. Dynamic behaviors of vimentin induced by interaction with GlcNAc molecules. *Glycobiology* **2012**, *22* (12), 1741−1759.
(30) Manouchehri, J. M.; Datta, J.; Marcho, L. M.; Reardon, J. J.; Stover, D.; Wesolowski, R.; Borate, U.; Cheng, T. Y. D.; Schnell, P. M.; Ramaswamy, B.; Sizemore, G. M.; Rubinstein, M. P.; Cherian, M. A. The role of heparan sulfate in enhancing the chemotherapeutic response in triple-negative breast cancer. *Breast Cancer Res.* **2024**, *26* (1), 153.
(31) Nozaki, I.; Ishikawa, N.; Miyanari, Y.; Ogawa, K.; Tagawa, A.; Yoshida, S.; Munekane, M.; Mishiro, K.; Toriba, A.; Nakayama, M.; Fuchigami, T. Borealin-Derived Peptides as Survivin-Targeting Cancer Imaging and Therapeutic Agents. *Bioconjugate Chem.* **2022**, *33* (11), 2149−2160.
(32) Lundquist, J. J.; Toone, E. J. The Cluster Glycoside Effect. *Chem. Rev.* **2002**, *102* (2), 555−578.
(33) Delaveris, C. S.; Chiu, S. H.; Riley, N. M.; Bertozzi, C. R. Modulation of immune cell reactivity with cis-binding Siglec agonists. *Proc. Natl. Acad. Sci. U. S. A.* **2021**, *118* (3), No. e2012408118.
(34) Lin, J.; Tang, H.; Jin, X.; Jia, G.; Hsieh, J. T. p53 regulates Stat3 phosphorylation and DNA binding activity in human prostate cancer cells expressing constitutively active Stat3. *Oncogene* **2002**, *21*, 3082−3088.
(35) Huang, S. W.; Chyuan, I. T.; Shiue, C.; Yu, M. C.; Hsu, Y. F.; Hsu, M. J. Lovastatin-mediated MCF-7 cancer cell death involves LKB1-AMPK-p38MAPK-p53-survivin signalling cascade. *J. Cell. Mol. Med.* **2020**, *24* (2), 1822−1836.
(36) Go, R. E.; Seong, S. M.; Choi, Y.; Choi, K. C. A Fungicide, Fludioxonil, Formed the Polyploid Giant Cancer Cells and Induced Metastasis and Stemness in MDA-MB-231 Triple-Negative Breast Cancer Cells. *Int. J. Mol. Sci.* **2024**, *25* (16), No. 9024.
(37) Hoppe-Seyler, F.; Butz, K. Repression of endogenous p53 transactivation function in HeLa cervical carcinoma cells by human papillomavirus type 16 E6, human mdm-2, and mutant p53. *J. Virol.* **1993**, *67* (6), 3111−3117.

https://doi.org/10.1021/acsomega.5c02098
ACS Omega XXXX, XXX, XXX−XXX